New Insights in Optimal Pilot Symbol Patterns for OFDM Systems

Michal Šimko[1], Paulo S. R. Diniz[2], Qi Wang[1] and Markus Rupp[1]

[1] Institute of Telecommunications, Vienna University of Technology, Vienna, Austria
[2] DEL POLI/UFRJ, PEE COPPE/UFRJ, Universidade Federal do Rio de Janeiro, Rio de Janeiro, Brazil
Email: msimko@nt.tuwien.ac.at
Web: http://www.nt.tuwien.ac.at/ltesimulator

***Abstract*—Nowadays, most wireless communication systems utilize coherent detection which implies the necessity of multiplexing reference symbols between data-symbols for the purpose of channel estimation. In Long Term Evolution (LTE), these reference symbols can consume up to 14.2% of the total bandwidth. In this work, we search for an optimal pilot-symbol pattern design using a post-equalization Signal to Interference and Noise Ratio (SINR) framework. We show how close to optimally choose the distance between adjacent pilot-symbols and how to distribute the available power between pilot and data symbol at the same time. We confirm the performance of our analytical solution by means of simulation. Compared to a system with a fixed distance between pilot-symbol and unit power distribution, the proposed system configuration yields a gain of around 30% in terms of capacity.**

***Index Terms*—LTE, Power distribution, OFDM, MIMO.**

I. Introduction

Coherent detection is widely utilized in current systems for mobile wireless communications. One of the most important aspects of such a system is its pilot-symbol pattern. In this paper, we analyze state-of-the-art knowledge about pilot-symbol patterns and provide a novel design that maximizes an approximation of the capacity.

A. Related Work

In the past, many researchers tried to find an optimal pilot-symbol pattern design using various criterions. In [1, 2], the authors chose the Mean Square Error (MSE) of a channel estimator as the cost function for the design of the pilot-symbol patterns. They showed that equipowered, equispaced pilot-symbols led to the lowest MSE. Authors of [3, 4] proposed a design pattern that maximized the system's capacity. There are many different approaches for designing pilot-symbol patterns based on the minimization of Bit Error Ratio (BER) [5] or Symbol Error Ratio (SER) [6].

Authors of [7–10] showed how to distribute available power among data and pilot-symbols given a certain pilot-symbol pattern. The authors utilized the post-equalization Signal to Interference and Noise Ratio (SINR) under imperfect channel knowledge as the cost function to solve the formulated problem. This relatively simple framework allows to treat the problem analytically and to find a solution independent of the actual channel realization.

B. Contribution

The main contributions of this paper are:

- By maximizing an approximation of the channel capacity, we derive the optimal distance between adjacent pilot-symbols in block fading scenarios and at the same time the optimal power distribution between pilot and data symbols.
- As with our previous work, all data, tools, as well implementations needed to reproduce the results of this paper can be downloaded from our homepage [11].

The remainder of the paper is organized as follows. In Section II, we describe the mathematical system model for transmitting pilots and data over a Multiple Input Multiple Output (MIMO) channel. In Section III, we briefly describe the post-equalization SINR expression for Zero Forcing (ZF) equalizers with imperfect channel knowledge. In Section IV, we summarize relevant knowledge about the performance of linear channel estimators. We formulate the optimization problem for optimal pilot-symbol design in Section V. Finally, we present simulation results in Section VI and conclude our paper in Section VII.

II. System Model

In this section, we briefly introduce a transmission model suitable for our further derivation. A received symbol in the frequency domain of an Orthogonal Frequency Division Multiplexing (OFDM) system at the n_{r}-th receive antenna can be written as

$$\tilde{\mathbf{y}}_{n_{\mathrm{r}}} = \sum_{n_{\mathrm{t}}=1}^{N_{\mathrm{t}}} \tilde{\mathbf{H}}_{n_{\mathrm{t}},n_{\mathrm{r}}} \mathbf{x}_{n_{\mathrm{t}}} + \tilde{\mathbf{n}}_{n_{\mathrm{r}}}, \tag{1}$$

where $\tilde{\mathbf{H}}_{n_{\mathrm{t}},n_{\mathrm{r}}} \in \mathbb{C}^{N_{\mathrm{sub}} \times N_{\mathrm{sub}}}$ represents the channel matrix in the frequency domain between the n_{t}-th transmit and the n_{r}-th receive antennas. The transmitted signal vector is referred to as $\mathbf{x}_{n_{\mathrm{t}}}$, the received signal vector as $\tilde{\mathbf{y}}_{n_{\mathrm{r}}}$. The vector $\tilde{\mathbf{n}}_{n_{\mathrm{r}}} \in \mathbb{C}^{N_{\mathrm{sub}} \times 1}$ denotes additive white zero mean Gaussian noise with variance σ_n^2 on an antenna n_{r}. In the case of a time-invariant channel, the channel matrix $\tilde{\mathbf{H}}_{n_{\mathrm{t}},n_{\mathrm{r}}}$ appears as a diagonal matrix. In this paper, we limit our discussion to the time-invariant case.

Specifically, the vector $\mathbf{x}_{n_\mathrm{t}} \in \mathbb{C}^{N_\mathrm{sub}\times 1}$ in Equation (1) comprises the precoded data symbols $\mathbf{x}_{\mathrm{d},n_\mathrm{t}} \in \mathbb{C}^{N_\mathrm{d}\times 1}$ and the pilot-symbols $\mathbf{x}_{\mathrm{p},n_\mathrm{t}} \in \mathbb{P}^{N_\mathrm{p}\times 1}$ from the set of all possible pilot-symbols $\mathbb{P}$ defined in Long Term Evolution (LTE), at the n_t-th transmit antenna placed by a suitable permutation matrix $\mathbf{P}$

$$\mathbf{x}_{n_\mathrm{t}} = \mathbf{P}\ \left[\mathbf{x}_{\mathrm{p},n_\mathrm{t}}^\mathrm{T}\ \mathbf{x}_{\mathrm{d},n_\mathrm{t}}^\mathrm{T}\right]^\mathrm{T}. \tag{2}$$

Figure 1 shows an example with the pilot-symbols multiplexed between the data symbols, where every D-th symbol is a pilot-symbol.

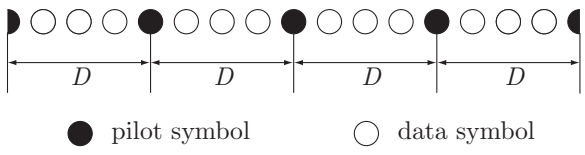

Fig. 1. Pilot pattern with equidistant reference symbols represented by black dots multiplexed within available resources with distance D.

The precoding process on a subcarrier k can be described as

$$\left[x_{\mathrm{d},1,k}\cdots x_{\mathrm{d},N_\mathrm{t},k}\right]^\mathrm{T} = \mathbf{W}_k\left[s_{1,k}s_{2,k}\cdots s_{N_\mathrm{l},k}\right]^\mathrm{T}, \tag{3}$$

where $x_{\mathrm{d},n_\mathrm{t},k}$ is a precoded data symbol at the n_t-th transmit antenna port and the k-th subcarrier, $\mathbf{W}_k \in \mathbb{C}^{N_\mathrm{t}\times N_\mathrm{l}}$ is a unitary precoding matrix at the k-th subcarrier and $s_{n_\mathrm{l},k} \in \mathbb{D}^{1\times 1}$ is the data symbol of the n_l-th layer at the k-th subcarrier. Here, $\mathbb{D}$ is the set of available modulation alphabets. The data elements from Equation (3) are stacked into a vector to form a data symbol vector $\mathbf{x}_{\mathrm{d},n_\mathrm{t}}$.

For the derivation of the post-equalization SINR, we use a MIMO input-output relation at the subcarrier level, given as:

$$\mathbf{y}_k = \mathbf{H}_k\mathbf{W}_k\mathbf{s}_k + \mathbf{n}_k. \tag{4}$$

The matrix $\mathbf{H}_k \in \mathbb{C}^{N_\mathrm{r}\times N_\mathrm{t}}$ denotes the MIMO channel matrix at the k-th subcarrier. This matrix is obtained by means of the Fourier transformation of the physical channel in the time domain. The vector $\mathbf{s}_k$ consists of the data symbols of all layers at the k-th subcarrier. The vector $\mathbf{n}_k$ represents additive white zero-mean Gaussian noise with variance σ_n^2 at a subcarrier k. We denote the effective channel matrix by

$$\mathbf{G}_k = \mathbf{H}_k\mathbf{W}_k. \tag{5}$$

Furthermore, the average power transmitted on each of the N_l layers is denoted by σ_s^2. The power transmitted on each data position is σ_d^2, while it is σ_p^2 on each pilot position.

III. Post-equalization SINR

In this section, we consider a time-invariant scenario and briefly describe an analytical expression for the post-equalization SINR of a MIMO system using a ZF equalizer based on imperfect channel knowledge. More details can be found in our previous work [9].

If perfect channel knowledge is available at the equalizer, the ZF estimate of the data symbol $\mathbf{s}_k$ is given as

$$\hat{\mathbf{s}}_k = \left(\mathbf{G}_k^\mathrm{H}\mathbf{G}_k\right)^{-1}\mathbf{G}_k^\mathrm{H}\mathbf{y}_k. \tag{6}$$

The data estimate $\hat{\mathbf{s}}_k$ defined in Equation (6) results in a post-equalization SINR of the m-th layer given as [12, 13]

$$\gamma_{m,k} = \frac{\sigma_s^2}{\sigma_n^2\mathbf{e}_m^\mathrm{H}\left(\mathbf{G}_k^\mathrm{H}\mathbf{G}_k\right)^{-1}\mathbf{e}_m}, \tag{7}$$

where the vector $\mathbf{e}_m$ is an $N_\mathrm{l}\times 1$ zero vector with a one on the m-th element. This vector extracts the signal on the corresponding layer m after the equalizer.

Let us proceed to the case of imperfect channel knowledge. We define the perfect channel as the channel estimate plus the error matrix due to the imperfect channel estimation

$$\mathbf{H}_k = \hat{\mathbf{H}}_k + \mathbf{E}_k, \tag{8}$$

where the elements of the matrix $\mathbf{E}_k$ are random variables, statistically independent of each other with zero mean and variance σ_e^2. Inserting Equation (8) in Equation (4), the input-output relation changes to

$$\mathbf{y}_k = \left(\hat{\mathbf{H}}_k + \mathbf{E}_k\right)\mathbf{W}_k\mathbf{s}_k + \mathbf{n}_k. \tag{9}$$

Since the channel estimation error matrix $\mathbf{E}_k$ is unknown at the receiver, the ZF solution is given again by Equation (6), but the channel matrix $\mathbf{H}_k$ is replaced by its estimate $\hat{\mathbf{H}}_k$, which is known at the receiver

$$\hat{\mathbf{s}}_k = \left(\hat{\mathbf{G}}_k^\mathrm{H}\hat{\mathbf{G}}_k\right)^{-1}\hat{\mathbf{G}}_k^\mathrm{H}\mathbf{y}_k, \tag{10}$$

with the matrix $\hat{\mathbf{G}}_k$ being equal to $\hat{\mathbf{H}}_k\mathbf{W}_k$.

Applying a ZF equalizer, Equation (10) leads to the SINR on the m-th layer [9]

$$\gamma_{m,k} = \frac{\sigma_s^2}{\left(\sigma_n^2 + \sigma_e^2\sigma_\mathrm{d}^2\right)\mathbf{e}_m^\mathrm{H}\left(\hat{\mathbf{G}}_k^\mathrm{H}\hat{\mathbf{G}}_k\right)^{-1}\mathbf{e}_m}. \tag{11}$$

IV. Channel Estimation

In this section, we summarize relevant knowledge about channel estimation under time-invariant channels. Although we limit our discussion only to a Least Squares (LS) channel estimator, note that based on the results shown in [9], all concepts can be easily applied also to other linear channel estimators.

It has been shown that equidistant pilot-symbols are optimal in terms of capacity and MSE [1, 2]. Therefore, we consider equidistant pilot patterns with distance D between adjacent pilots. An example of such a pattern is shown in Figure 1.

MSE of a linear channel estimator can be expressed as [9]

$$\tilde{\sigma}_e^2 = c_e\left(D\right)\frac{\sigma_n^2}{\sigma_\mathrm{p}^2} + d\left(D\right), \tag{12}$$

where $c_e\left(D\right)$ and $d\left(D\right)$ are real constants depending on the distance D between adjacent pilot-symbols that determine the performance of the channel estimators.

The coefficient $c_e(D)$ from Equation (12) is purely determined by the pilot-symbol pattern and the coefficient $d(D)$ is additionally dependent on the channel autocorrelation function [9]. Figure 2 shows the behavior of these coefficients over distance between two adjacent pilot-symbols. Let us first consider $c_e(D)$. At low distances it grows rapidly with increasing distance between two pilot-symbols. At rather large distances, it remains almost constant. The value of the coefficient $d(D)$ is first close to zero and once after the distance between two pilots is greater than the coherence bandwidth of the channel, it grows with increasing distance between two pilot-symbols.

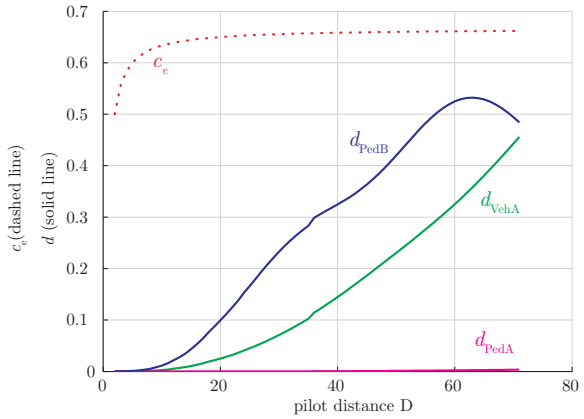

Fig. 2. Coefficients $c_e(D)$ and $d(D)$ over distance between two adjacent pilot-symbols for an LS channel estimator for various ITU channel models.

Inserting Equation (12) into Equation (11), assuming that available transmit power is evenly distributed between all layers $\sigma_s^2 = \frac{\sigma_{\mathrm{d}}^2}{N_{\mathrm{l}}}$ and simplifying the expression, we obtain the SINR expression:

$$\gamma_{m,k} = \frac{1}{N_{\mathrm{l}}\mathbf{e}_m^{\mathrm{H}}\left(\mathbf{G}_k^{\mathrm{H}}\mathbf{G}_k\right)^{-1}\mathbf{e}_m} f\left(\sigma_{\mathrm{p}}^2, \sigma_{\mathrm{d}}^2, D\right), \tag{13}$$

for which the power allocation function $f\left(\sigma_{\mathrm{p}}^2, \sigma_{\mathrm{d}}^2, D\right)$ is given as

$$f\left(\sigma_{\mathrm{p}}^2, \sigma_{\mathrm{d}}^2, D\right) = \frac{1}{\sigma_n^2\left(\frac{1}{\sigma_{\mathrm{d}}^2} + \frac{c_e(D)}{\sigma_{\mathrm{p}}^2}\right) + d(D)}. \tag{14}$$

Note that the power allocation function is independent of the channel realization. In this work, we consider the case, when the available transmit power is utilized. Therefore, we introduce a variable p_{off} is defined as the power offset between the power of the pilot-symbols and the data symbols, denoted by

$$\sigma_{\mathrm{d}}^2 = p_{\mathrm{off}}\sigma_{\mathrm{p}}^2. \tag{15}$$

When transmitting the available transmit power, the powers transmitted at the pilot and the data symbols are interconnected as

$$\sigma_{\mathrm{d}}^2 N_{\mathrm{d}} + \sigma_{\mathrm{p}}^2 N_{\mathrm{p}} = N_{\mathrm{d}} + N_{\mathrm{p}}, \tag{16}$$

where N_{d} and N_{p} are numbers of the data and pilot-symbols, respectively. With Equation (15) and Equation (16), the power allocation function depends only on the power offset p_{off} and the distance between adjacent pilot-symbols D, therefore from now on, it is denoted by $f(p_{\mathrm{off}}, D)$.

V. Pilot Design

In this section, we analyze pilot-symbol patterns using a post-equalization SINR framework. In general, certain amount of resources like bandwidth and power are available for transmission of data and pilot-symbols. If more resources are used for data transmission, there is less left for the transmission of the pilot-symbols, leading to a degradation of the channel estimation performance. Clearly, there is an equilibrium for the distribution of the available resources.

The optimal distance between two adjacent pilot-symbols and power distribution between pilot and data symbols cannot be found exclusively by maximizing the post-equalization SINR. This would lead to a solution with small distance between adjacent pilot-symbols, which would decrease the available bandwidth for data transmission. Therefore, another type of cost function is required that allows to include a penalty due to the bandwidth occupied by the pilot-symbols. Capacity is one of the possible choices for the new cost function

$$\mathcal{C} = B\log_2(1+\gamma_m), \tag{17}$$

where B is the bandwidth utilized for the data transmission. Inserting the post-equalization SINR into the capacity expression allows to consider the effect of the channel estimation error and power allocation in a very simple way [14]. The post-equalization SINR Equation (13) can be multiplicatively decomposed into two parts, the channel independent power allocation function Equation (14) and a function that depends on the actual channel $f_h(\mathbf{G}) = \frac{1}{N_{\mathrm{l}}\mathbf{e}_m^{\mathrm{H}}\left(\mathbf{G}_k^{\mathrm{H}}\mathbf{G}_k\right)^{-1}\mathbf{e}_m}$. In order to maximize the system's capacity without taking into account an actual channel realization, we approximate Equation (17) at high SINR by

$$\begin{aligned}\mathcal{C} &\approx B\log_2\left(f(p_{\mathrm{off}}, D) f_h(\mathbf{G})\right) \\ &\approx B\log_2\left(f(p_{\mathrm{off}}, D)\right) + B\log_2\left(f_h(\mathbf{G})\right)\end{aligned} \tag{18}$$

and at low Signal to Noise Ratio (SNR) by

$$\mathcal{C} \approx \log_2(e)\, B f(p_{\mathrm{off}}, D) f_h(\mathbf{G}). \tag{19}$$

The only part influenced by changing the distance between pilots and by adjusting the power allocation is $B\log_2\left(f(p_{\mathrm{off}}, D)\right)$ for high SNR and $Bf(p_{\mathrm{off}}, D)$ for low SNR values, respectively. Therefore, we define the cost function as

$$f_{\mathrm{cost}}(p_{\mathrm{off}}, D) = \begin{cases} Bf(p_{\mathrm{off}}, D) & ;\mathrm{SNR} < \mathrm{SNR}_{\mathrm{tr}} \\ B\log_2\left(f(p_{\mathrm{off}}, D)\right) & ;\mathrm{SNR} > \mathrm{SNR}_{\mathrm{tr}} \end{cases} \tag{20}$$

where $\mathrm{SNR}_{\mathrm{tr}}$ is an SNR threshold value, at which the capacity approximation for low SNR values is replaced by that at high

SNR values. With the above defined cost function, we can formulate our optimization problem as

$$\begin{aligned} \underset{p_{\text{off}},D}{\text{maximize}} \quad & f_{\text{cost}}\left(p_{\text{off}}, D\right) \\ \text{subject to} \quad & N_{\text{d}}\sigma_{\text{d}}^2 + N_{\text{p}}\sigma_{\text{p}}^2 = N_{\text{d}} + N_{\text{p}} \\ & B = \text{const} \end{aligned} \tag{21}$$

For a fixed distance D, the optimal value of power distribution p_{off} can be efficiently found employing techniques of convex optimization. For solving the optimization problem in Equation (21) we utilized CVX, a package for specifying and solving convex programs [15, 16]. After finding optimal values of the variable p_{off} for all possible distances D, we maximize the cost function in order to find the optimal combination of the variables p_{off} and D.

Figure 3 depicts example of the cost function at an SNR of 20 dB with the VehA channel model.

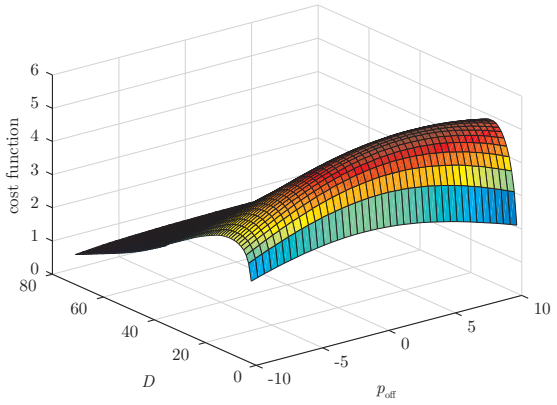

Fig. 3. Cost function plotted over pilot distance D between adjacent pilot-symbols and different power offset p_{off} between pilot and data symbols for SNR= 20dB and VehA channel model.

Figure 4 shows the optimal choice of distance between adjacent pilot-symbols and the corresponding power offset between data and pilot-symbols over SNR for various ITU channel models. With increasing SNR, a better channel estimate is required, therefore the optimal distance between neighboring pilot-symbols is decreasing. At the same time, the power offset between pilot and data symbols is decreasing with increasing SNR, which corresponds to less and less power assigned to the pilot-symbols, since there is less noise at the pilot-symbols.

VI. Simulation Results

In this section, we present simulation results and compare the transmission system's capacity setting an optimal distance between adjacent pilot-symbols and with optimal power distribution between pilot and data symbols, against a system using fixed distance between pilot-symbols and unit distribution of power between data and pilot-symbols. All data, tools and scripts are available online [11] in order to allow other researchers to reproduce the results shown in this paper. Table I shows the most important simulator settings.

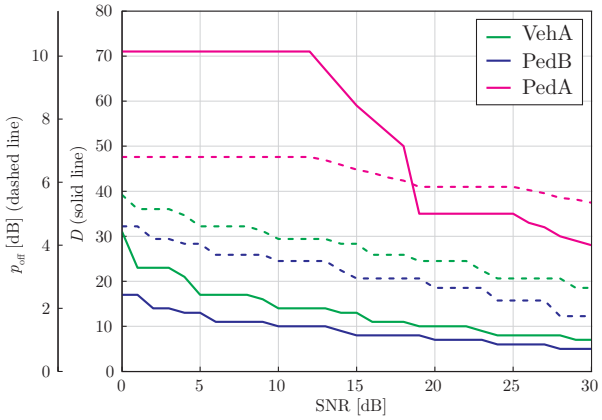

Fig. 4. Optimal choice of the distance between adjacent pilot-symbols D and the optimal power offset between data and pilot-symbols p_{off} over SNR for various ITU channel models.

TABLE I
Simulator Settings for Fast Fading Simulations

Parameter	Value
Bandwidth	1.4 MHz
Number of transmit antennas	1
Number of receive antennas	1
Receiver type	ZF
Transmission mode	Open-loop spatial multiplexing
Channel type	ITU VehA, PedA, PedB [17]

Figure 5 shows capacity over distance between adjacent pilot-symbols D and over variable p_{off} at SNR = 20 dB. We observe that the capacity maximum matches with the maximum of the cost function in Figure 3.

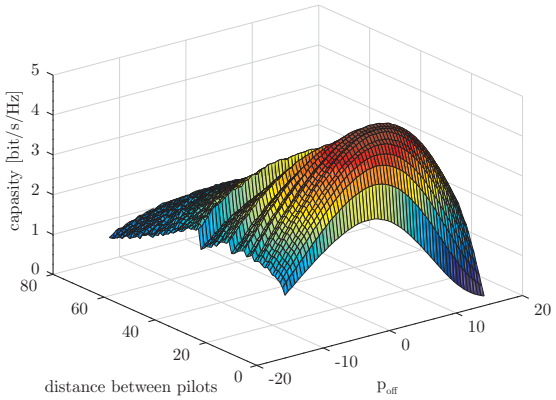

Fig. 5. System's capacity plotted over pilot distance D between adjacent pilot-symbols and different power offset p_{off} between pilot and data symbols for SNR= 20dB and VehA channel model.

Capacities of two different systems are compared in Figure 6. The solid lines represent a system using the optimal distance between adjacent pilot-symbols and optimal power distribution between pilot and data symbols. Optimal values for both of the variables are shown in Figure 4. The dashed line in Figure 6 represents a system using fixed distance between adjacent pilot-symbols $D = 3$ and no power distribution

between pilot and data symbols. We chose $D = 3$, because this is the distance used in an LTE system [18]. Note, that the gain achieved for one OFDM symbol will not be achieved by the subframe structure utilized by LTE systems, consisting of more OFDM symbols, in which some of the OFDM symbols do not carry any reference symbols.

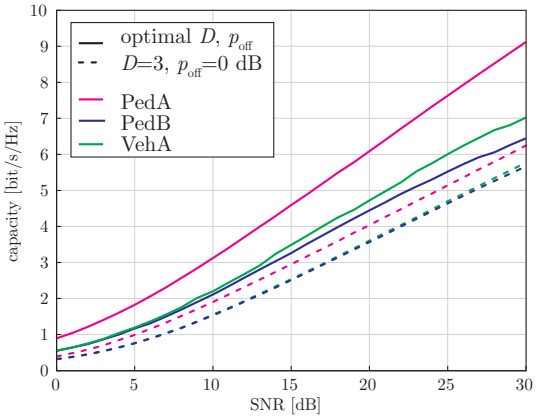

Fig. 6. Capacity versus SNR for system with optimal pilot distance D between pilot-symbols and optimal power offset p_{off} (solid line) and for system with fixed distance between pilot-symbols ($D = 3$) and no power distribution (dashed line).

VII. Conclusion

In this paper, we tackled the problem of optimal pilot-symbol design for time-invariant scenarios. We delivered analytical expressions for the optimal distance between adjacent pilot-symbols and the optimal power distribution between pilot-symbols and data symbols. The optimal values were confirmed by means of simulations and compared to a system using a fixed distance between adjacent pilot-symbols and unit power distribution. Such system is outperformed by an optimal system by approximately 30% in terms of capacity. Note that we considered only single OFDM symbol, therefore the gain is smaller, when using subframe structure, where some OFDM symbols do not carry any pilot-symbols. In this paper, we showed that at low SNR values the number of necessary pilot-symbols can be decreased, but their power have to be significantly increased compared to the power of the data symbols. On other hand, in order to obtain optimal system performance at high SNR values, pilot-symbols pattern with higher density have to be utilized, though with smaller power offset.

Acknowledgments

The authors would like to thank the LTE research group for continuous support and lively discussions. This work has been funded by the Christian Doppler Laboratory for Wireless Technologies for Sustainable Mobility, KATHREIN-Werke KG, and A1 Telekom Austria AG. The financial support by the Federal Ministry of Economy, Family and Youth and the National Foundation for Research, Technology and Development is gratefully acknowledged. They are also thankful to CNPq and FAPERJ for their financial support of the second author.

References

[1] R. Negi and J. Cioffi, "Pilot Tone Selection for Channel Estimation in a Mobile OFDM System," *IEEE Transactions on Consumer Electronics*, vol. 44, no. 3, pp. 1122–1128, 1998.

[2] I. Barhumi, G. Leus, and M. Moonen, "Optimal Training Design for MIMO OFDM Systems in Mobile Wireless Channels," *IEEE Transactions on Signal Processing*, vol. 51, no. 6, pp. 1615–1624, 2003.

[3] B. Hassibi and B.M. Hochwald, "How much Training is needed in Multiple-Antenna Wireless Links?," *IEEE Transactions on Information Theory*, vol. 49, no. 4, pp. 951–963, 2003.

[4] S. Adireddy, L. Tong, and H. Viswanathan, "Optimal Placement of Training for Frequency-Selective Block-Fading Channels," *IEEE Transactions on Information Theory*, vol. 48, no. 8, pp. 2338–2353, 2002.

[5] W. Zhang, X.G. Xia, and PC Ching, "Optimal Training and Pilot Pattern Design for OFDM Systems in Rayleigh Fading," *IEEE Transactions on Broadcasting*, vol. 52, no. 4, pp. 505–514, 2006.

[6] X. Cai and G.B. Giannakis, "Error Probability Minimizing Pilots for OFDM with M-PSK Modulation over Rayleigh-Fading Channels," *IEEE Transactions on Vehicular Technology*, vol. 53, no. 1, pp. 146–155, 2004.

[7] M. Šimko, S. Pendl, S. Schwarz, Q. Wang, J. C. Ikuno, and M. Rupp, "Optimal Pilot Symbol Power Allocation in LTE," in *Proc. 74th IEEE Vehicular Technology Conference (VTC2011-Fall)*, San Francisco, USA, Sept. 2011.

[8] M. Šimko and M. Rupp, "Optimal Pilot Symbol Power Allocation in Multi-Cell Scenarios of LTE," in *Conference Record of the Fourtyfifth Asilomar Conference on Signals, Systems and Computers, 2011*, Pacific Grove, USA, Nov. 2011.

[9] M. Šimko, Q. Wang, and M. Rupp, "Optimal Pilot Symbol Power Allocation under Time-variant Channels," *EURASIP Journal on Wireless Communications and Networking*, 2012, http://jwcn.eurasipjournals.com/content/2012/1/225/abstract.

[10] M. Šimko, P. S. R. Diniz, Q. Wang, and M. Rupp, "Power Efficient Pilot Symbol Power Allocation under Time-variant Channels," in *Proc. 76th IEEE Vehicular Technology Conference (VTC2012-Fall)*, Quebec, Canada, Sept. 2012.

[11] "LTE simulator homepage," [online] http://www.nt.tuwien.ac.at/ltesimulator/.

[12] A. Hedayat, A. Nosratinia, and N. Al-Dhahir, "Linear Equalizers for Flat Rayleigh MIMO Channels," in *Proc. of IEEE ICASSP 2005*, Mar. 2005, vol. 3, pp. iii/445 – iii/448 Vol. 3.

[13] M. Rupp, "Robust Design of Adaptive Equalizers," *IEEE Transactions on Signal Processing*, vol. 60, no. 4, pp. 1612 –1626, Apr. 2012.

[14] S. Schwarz, M. Šimko, and M. Rupp, "On performance bounds for MIMO OFDM based wireless communication systems," in *Signal Processing Advances in Wireless Communications SPAWC 2011*, San Francisco, CA, June 2011, pp. 311 –315.

[15] Inc. CVX Research, "CVX: Matlab software for disciplined convex programming, version 2.0 beta," http://cvxr.com/cvx, Sept. 2012.

[16] M. Grant and S. Boyd, "Graph Implementations for Nonsmooth Convex Programs," in *Recent Advances in Learning and Control*, V. Blondel, S. Boyd, and H. Kimura, Eds., Lecture Notes in Control and Information Sciences, pp. 95–110. Springer-Verlag Limited, 2008, http://stanford.edu/~boyd/graph_dcp.html.

[17] ITU, "Recommendation ITU-R M.1225: Guidelines for evaluation of radio transmission technologies for IMT- 2000 systems," Recommendation ITU-R M.1225, International Telecommunication Union, 1998.

[18] 3GPP, "Evolved Universal Terrestrial Radio Access (E-UTRA); Physical channels and modulation," TS 36.211, 3rd Generation Partnership Project (3GPP), Sept. 2008.